Environmental Science & Technology

pubs.acs.org/est

Article

Plastic biodegradation: Do *Galleria mellonella* Larvae Bioassimilate Polyethylene? A Spectral Histology Approach Using Isotopic Labeling and Infrared Microspectroscopy

Agnès Réjasse,* Jehan Waeytens, Ariane Deniset-Besseau, Nicolas Crapart, Christina Nielsen-Leroux, and Christophe Sandt*

Cite This: https://doi.org/10.1021/acs.est.1c03417

Read Online

ACCESS | Metrics & More | Article Recommendations | Supporting Information

ABSTRACT: Environmental pollution by the nearly nonbiodegradable polyethylene (PE) plastics is of major concern; thus, organisms capable of biodegrading PE are required. The larvae of the Greater Wax Moth, *Galleria mellonella* (Gm), were identified as a potential candidate to digest PE. In this study, we tested whether PE was metabolized by Gm larvae and could be found in their tissues. We examined the implication of the larval gut microbiota by using conventional and axenic reared insects. First, our study showed that neither beeswax nor LDPE alone favor the growth of young larvae. We then used Fourier transform infrared microspectroscopy (μFTIR) to detect deuterium in larvae fed with isotopically labeled food. Deuterated molecules were found in tissues of larvae fed with deuterium labeled oil for 24 and 72 h, proving that μFTIR can detect metabolization of 1 to 2 mg of deuterated food. Then, Gm larvae were fed with deuterated PE (821 kDa). No bioassimilation was detected in the tissues of larvae that had ingested 1 to 5 mg of deuterated PE in 72 h or in 19 days, but micrometer sized PE particles were found in the larval digestive tract cavities. We evidenced weak biodegradation of 641 kDa PE films in contact for 24 h with the dissected gut of conventional larvae and in the PED4 particles from excreted larval frass. Our study confirms that Gm larvae can biodegrade HDPE but cannot necessarily metabolize it.

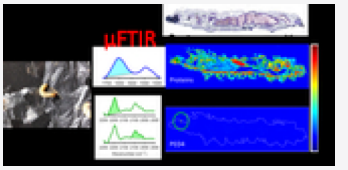

KEYWORDS: *polyethylene, plastic degradation, biodegradation, Galleria mellonella larvae, FTIR microspectroscopy, isotopic labeling, hyperspectral imaging*

INTRODUCTION

Due to high production, inefficient waste collection and long lifetime, plastics are now a major cause of environmental pollution in land and maritime environments.[1] Development of new biodegradable plastics and new plastic degradation processes are pursued to remediate these problems. Biodegradation would offer advantages over other methods (landfill storage, incineration, chemical degradation) as it can be more environmentally friendly, produces less waste, and reduces the cost of waste management. Polyethylene (PE), one of the most produced plastics, is considered almost nonbiodegradable. PE is synthesized in many forms with various molecular weights (MW): PE wax (MW < 1000 Da), linear low-density PE (LLDPE), low density PE (LDPE), and high density PE (HDPE with MW of several millions of Da). They differ by their molecular weights, chain lengths, degrees of branching, packing densities, and crystallinities which affect biotic degradation. Biodegradation is slower for PE with lower branching, higher crystallinity, and chain lengths for HDPE. Hydrophobic surface properties, glass transition temperature (chain mobility), and long-range structure (surface area etc.) may also affect biodegradation. Furthermore, to increase its lifetime, PE is generally synthesized with antioxidants and UV stabilizers.[2] Modest biodegradation rates were reported in the literature by microorganisms from natural microbial communities.[3−6]

Another potential plastic biodegradation method reported in the literature is the use of insect larvae or their commensal gut microorganisms.[7−13] Several recent studies reported degradation of PE by the caterpillars of the Greater Wax Moth *Galleria mellonella* (Gm).[11,12,14−16] There is a rational motivation for the use of these larvae. The metabolic pathways involved in the degradation of long-chain hydrocarbons (like long-chain fatty acids) are expected to play an important role in the degradation of PE that is composed of a long aliphatic chain. Since, Gm larva feeds on and metabolizes long-chain hydrocarbons from beeswax,[17] it may also potentially metabolize PE. If this is the case, the role of gut enzymes and the gut microbiota should be assessed. However, involvement of the larval gut microbiota may be questionable. Recently, Kong et al.[14] reported PE biodegradation independent of the intestinal microbiota while Ren,[12] Cassone,[16] and

Received: May 27, 2021
Revised: November 26, 2021
Accepted: December 1, 2021

Lou[18] described the implication of various species from the Gm gut microbiota. In addition, the original study[11] reporting the degradation of PE by the Gm larva was criticized on several methodological points by Weber et al.[19] Indeed, the approach used to investigate the potential of the larvae to metabolize PE in those studies presents several issues: gut residues on the PE films are often misinterpreted for PE oxidation;[20] the ingestion of PE does not imply metabolization of the polymer, and PE metabolization by the larvae was never demonstrated. PE could be biodegraded by gut bacteria and yet not be metabolized by the larvae and not transformed into biological tissue. This and the controversial results about microbiota involvement make it necessary to further investigate whether Gm larvae and/or their microbiota can really biodegrade and metabolize PE.

In this study, we present a methodology capable of detecting the eventual metabolization of PE by Gm larvae. First, we tested whether PE can be used as an energy source and if it provided nutritional value for the Gm larvae. Then, we used Fourier transform infrared microspectroscopy (μFTIR) to perform hyperspectral imaging of cryo-sections of the whole larvae, and we evaluated the capability of Gm larvae to bioassimilate PE as well as its integration in the larval tissues. We developed an original protocol using polyethylene isotopically labeled with deuterium (PED4) to detect if deuterated molecules were metabolized in the Gm larval tissue after deuterated PE ingestion. Indeed, based on its infrared spectrum, the —CH_2— peak from PE cannot be distinguished from the —CH_2— peak from lipids in larva tissues at low concentrations, whereas —CD_2— from deuterated PE has specific absorption peaks in the infrared transparency window of the tissues and could be easily identified in the larvae. The large shift in peak positions between C−H and C−D is caused by the larger atomic mass of deuterium causing a strong shift in the vibration frequency of the C−D bonds. This method is one of the most relevant to reveal metabolization. Furthermore, PED4 and regular PE exhibit similar chemical and physical properties, and their biodegradation products are expected to be identical. After metabolization, PED4 should be found as deuterated molecules containing —CD_2— moieties, presumably in tissues containing long aliphatic chains molecules. Detecting —CD_2— groups in the tissues of the larvae should be a direct indication of PE metabolization. The sensitivity and relevance of the method were evaluated by feeding experiments with deuterated oil. The implication of the gut microbiota in the biodegradation process was evaluated using both conventional and axenically reared larvae (without microbiota). The PE nutritional value was evaluated by following larval growth with different diets at two development stages.

MATERIALS AND METHODS

PE Materials. Low density PE supermarket bags were used for insect feeding and growth experiments. High density PE bags were used for assessing the oxidation of PE in contact with the dissected Gm larva gut. Perdeuterated PE flakes (PED4) were purchased from Medical Isotopes Inc. (Pelham, NH, U.S.A.). The crystallinities X_c of the PEs used in this study were measured by FTIR spectroscopy using the method of Hagemann[21] and are described in the Supporting Information. We found a X_c of 0.83 for HDPE, a X_c of 0.68 for LDPE, and a X_c of 0.91 for PED4. The PEs used in this study were characterized by high-temperature gel permeation chromatography (HT-GPC) by the Peakexpert company (Tours, France). HT-GPC was performed at 150 °C in stabilized trichlorobenzene on Agilent Mixed-B columns. Columns were calibrated with polystyrene references. The average molecular weights were found as follows: LDPE bags Mn 40.7 kDa, Mw 249.0 kDa, Mz 679 kDa; HDPE bags Mn 34.2 kDa, Mw 641.1 kDa, Mz 4277 kDa; PED4Mn 139.7 kDa, Mw 821.7 kDa, Mz 3354 kDa. All samples presented large MW distributions ranging from hundreds to millions of Daltons. The molecular weight distributions of the three PE samples (LDPE bags, HDPE bags, and PED4) are shown in Supplementary Information (Figure S6).

Insect Rearing and Feeding. Gm larvae were produced on site in the insectarium at INRAE Micalis Institute at Jouy-en-Josas, France. Gm eggs were hatched at 27 °C, and the larvae were reared on beeswax and pollen (La Ruche Roannaise, Roanne, France) with a 12 h day/12 h night cycle in an MLR352H-PE Environmental Test Chamber (Panasonic Healthcare Co, Ltd. Japan). The feeding assays were performed in the dark.

The moths laid eggs on paper that were directly placed on pollen and covered with beeswax in closed aerated plastic boxes. For the axenic larvae, eggs were first sterilized by 10 min of exposure on each side with UV light at 254 nm and fed with gamma-ray sterilized pollen and beeswax in an autoclaved glass jar with an aerated lid covered by sterile gauze and carded cotton. The boxes and the jars were placed in an incubator at 27 °C, simulating the day−night cycle.

In order to verify that the larvae were axenic, 2 larvae were crushed and homogenized with a sterilized pestle in 500 μL of sterile physiological water, and 100 μL of the suspension were spread on a BHI Petri dish. No bacterial growth was observed after 7 days at 37 °C, and no bacterial 16S DNA was found following V3/V4 PCR;[22] for conventional larvae, 10^6 bacteria/larva were found.

Effect of Diet on Insect Growth. L2-L3 early stage larvae (20 mg each) were placed individually in 12-well plates and were either starved or fed *ad libitum* with one of five different diets: beeswax alone, pollen alone, LDPE alone, beeswax + pollen, or beeswax + LDPE. Six larvae were used for each diet for a total of 36 larvae. The food uptake was evaluated by weighing the remaining food. The larvae were kept at 27 °C and weighed individually every 2−3 days. The test was continued for 16 days until the larvae fed a beeswax + pollen diet reached stage L6.

A second test was carried out with another batch of 36 L6-larvae (last larval stage, 160 mg), 6 for each diet. The larvae were placed individually in 6-well plates at 27 °C and fed with LDPE as previously described. The larvae reached the chrysalis stage in 8−10 days; the test was carried out for an additional 12 days until the adult stage.

The average growth of the 6 larvae and the standard deviations were calculated with the "Origin Pro 2016" software (Origin lab, Northampton, MA).

Perdeuterated Oil Feeding. Five conventional and five axenic L6 stage larvae were starved for 24 h before free-feeding for 24 or 72 h with pollen soaked with perdeuterated oil with a density of 0.887 g/mL (*N*-hexadecane ($C_{16}D_{34}$, 98%), Cambridge Isotope Laboratories, Inc., U.S.A.). Larvae fed for 24 h each ingested 6.7 mg of pollen and 1.6 μL (1.4 mg) of oil; larvae fed for 72 h ingested each 20 mg of pollen and 4.8 μL (4.2 mg) of oil.

Perdeuterated Polyethylene (PED4) Feeding. PED4 was received in flakes of several millimeters cubed. PED4 films

https://doi.org/10.1021/acs.est.1c03417
Environ. Sci. Technol. XXXX, XXX, XXX−XXX

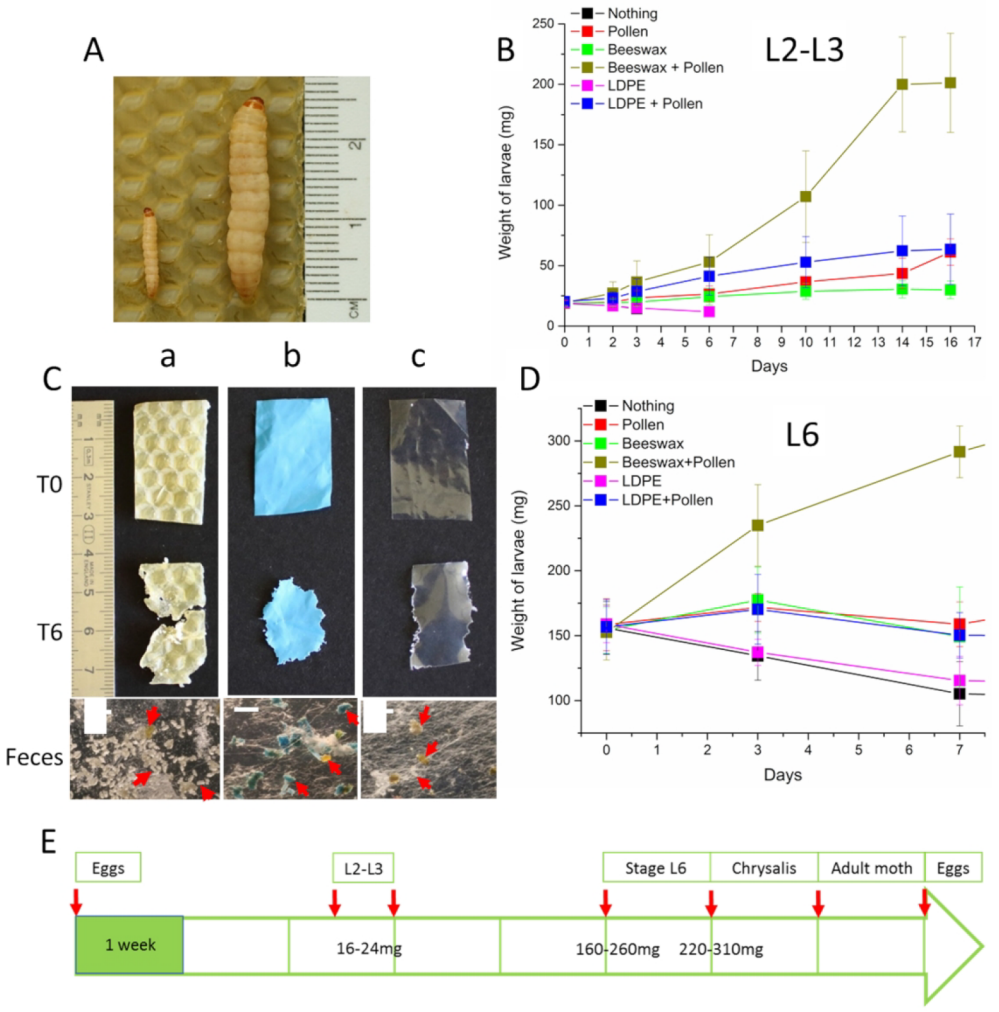

Figure 1. Evaluation of the nutritional value of different diets in Gm. (A) Gm larvae on beeswax: L2-L3 stage on the left, L6 stage on the right. (B) Growth curve of L2-L3 Gm larvae fed different diets. L2-L3 larvae ate 0.6 ± 0.3 and 2.5 ± 2.2 mg of LDPE per larva for the PE alone and PE +pollen diet, respectively. Larva fed PE alone died in 3 to 6 days. (C) Pictures evidencing the consumption of beeswax or LDPE at T0 and T6 (zero and 6 days) and the excretion of LDPE in feces. Arrows show the feces and PE fragments among the silk fibers. Scale bars: 2 mm. (D) Growth curve of last stage L6 Gm fed different diets. (E) Typical Gm larva evolution time scale (weeks) and larval weight (L2-L3 and L6) when fed with beeswax and pollen. Larvae were reared at 27 °C.

were prepared either by pressing PED4 flakes at 140 °C for 15−30 min in an in-house designed press giving 30 to 40 μm thick films or by pressing PED4 flakes at room temperature for 1 min at 15 ton/cm^2 in a Specac manual hydraulic press (Eurolabo, Paris, France).

Two batches of L6 stage larvae (5 axenic and 5 conventional) were starved for 24 h at 27 °C in individual boxes. The larvae were then allowed to feed freely on PED4 films for 3 days. The larvae were then killed by quick freezing and cryo-sectioned. The amount of PED4 ingested was evaluated by weighting the PED4 film left over, and feces were collected and stored at −80 °C for further evaluation. Only larvae fed with more than 1 mg of PED4 were analyzed by μFTIR. Three axenic and three conventional larvae were fed for up to 19−21 days with PED4 alternating with pollen to allow survival.

Cryo-sectioning and Preparation for Hyperspectral IR Imaging. The cryo-sections were prepared on the Abridge platform (INRAE, Jouy-en-Josas, France). The larvae were frozen in a SnapFrost system (Excilone, Elancourt, France) in isopentane at −80 °C and then stored at −80 °C. The 10 and 20 μm sagittal sections were cut at −20 °C with a Shandon FSE cryostat (ThermoFisher, Courtaboeuf, France). The 20 μm thick sections improved the sensitivity of the detection for the weak C−D peaks, but tissue lipid and protein peaks were saturated. Consecutive sections were made and deposited on different slide supports: on StarFrost (Knittelglass, Germany) for immediate cresyl-violet staining, on SuperFrost plus (ThermoFisher, France) for histological staining, and on IR-grade polished IR-transparent CaF_2 slides (Crystran, Poole, U.K.) for IR hyperspectral imaging. The sections on CaF_2 were stored in a desiccator under a continuous flow of nitrogen until analysis.

Hyperspectral FTIR Imaging. Fourier transform infrared hyperspectral images were recorded at the SMIS beamline, SOLEIL synchrotron, France, on a Cary 620 infrared microscope (Agilent, Courtaboeuf, France) equipped with a 128 × 128 pixel Lancer Focal Plane Array (FPA) detector and coupled to a Cary 670 spectrometer. Hyperspectral images were measured in transmission in the standard magnification mode with a 4×/0.2 NA Schwarzschild objective and matching condenser giving a field of view of 2640 × 2640 μm^2 and a

https://doi.org/10.1021/acs.est.1c03417
Environ. Sci. Technol. XXXX, XXX, XXX−XXX

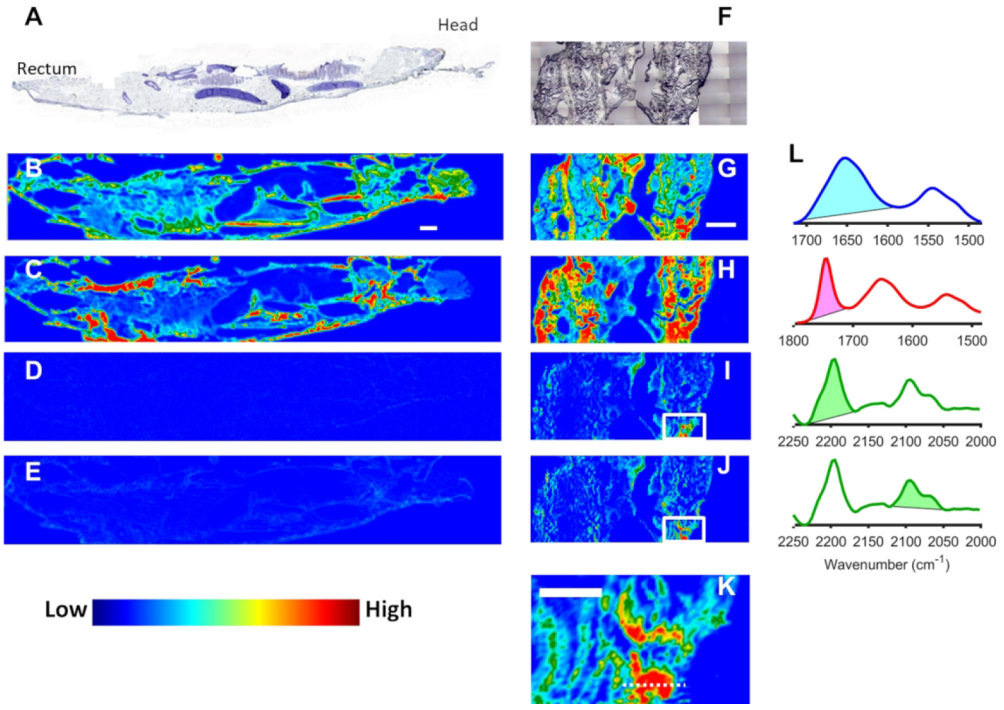

Figure 2. Spectral histology of Gm larvae and detection of C16D34 signal in larva sections. (A–E) Micrographs of a section of a control larva (4× magnification). (A) Bright field of cresyl violet stained section. (B–E) Infrared spectral histology maps showing the distribution of (B) proteins and (C) lipids; the absence of a C–D peak at (D) 2197 cm^{-1} and at (E) 2098 cm^{-1}. This shows that deuterium is not found in the control larva. (F–K) Micrographs of unstained larva fed for 72 h with C16D34 oil. (F) Bright field of the unstained section. (G–K) Infrared maps of (G) protein distribution and (H) lipid distribution. The detection of C–D peaks in the deuterated oil fed larvae is evidenced in (I) by the 2197 cm^{-1} C–D peak area from CD2 asymmetric stretching and in (J) by the 2098 cm^{-1} C–D peak area from CD2 symmetric stretching. (K) Zoom on a C–D-rich region delimited by the box in images I and J. Scale bars: 0.5 mm. (L) The peak area used for plotting the spectral maps, in descending order: protein amide I, lipid ester C═O, and symmetrical and asymmetrical C–D stretching peaks of the $C_{16}D_{34}$ oil.

projected pixel size of 20.4 × 20.4 μm^2. The actual spatial resolution of the images was evaluated by the step-edge method to be approximately 40 μm at 1545 cm^{-1} and 30 μm at 2915 cm^{-1}. Mosaics composed of several FPA tiles were recorded to image the whole sections.

Hyperspectral images were recorded between 900 and 3900 cm^{-1} at 8 cm^{-1} resolution, with 256 and 128 co-added scans for background and sample, respectively.

Synchrotron Radiation FTIR Microspectroscopy (SR-μFTIR). SR-μFTIR was performed at the SOLEIL synchrotron facility on the SMIS beamline.[23] The synchrotron was operated at 500 mA in top-up mode for injections. Spectra and maps of the sections were recorded using Continuum microscopes coupled to Nicolet 8700 or 5700 spectrometer (ThermoFisher, Courtaboeuf, France). The microscopes were equipped with 32×/0.65 NA Schwarzschild objectives and matching condensers and liquid-cooled narrow-band MCT/A detectors. The confocal aperture was set at 12 × 12 μm^2. Spectra were recorded in transmission mode at 6 cm^{-1} resolution with 16 to 32 scans between 650 and 4000 cm^{-1}.

Data Analysis. Spectral images were computed in ResolutionPro (Agilent) and in Quasar.[24,25] Spectral images were created using the baseline-corrected, integrated areas of the peaks of interest. Lipid and protein distributions were imaged by the C–H stretching peaks of CH_2 and CH_3 between 2800 and 3000 cm^{-1} and the amide I band between 1590 and 1705 cm^{-1}, respectively. The deuterated PE was detected and imaged by symmetric and asymmetric CD_2 stretching peaks at 2085 cm^{-1} (2030–2130 cm^{-1}) and 2190 cm^{-1} (2165–2230 cm^{-1}). The deuterium/protein peak area ratio was computed with protein band area integrated between 1480 and 1720 cm^{-1}. K-means clustering of the hyperspectral images and computation of Pearson correlation coefficients between peak-area ratios were performed in Quasar. K-means clustering is a multivariate pattern-recognition method that allows clustering spectra based on their similarities,; 10 runs and 300 iterations were used. Water vapor subtraction was performed in Matlab 2016 (MathWorks, Natick, MA) with an in-house script.

RESULTS

Nutritional Value of PE. To estimate the relative nutritional value of PE as an energy source for Gm, we compared the food uptake, weight gain, and larval survival for different diets: control (nothing), pollen alone, beeswax alone, beeswax + pollen, LDPE alone, and LDPE + pollen. We set up growth experiments with conventional larvae at two different stages (Figure 1A,E): young larvae (L2-L3 stage, 20 mg per larva) and last instar (L6 stage, 160 mg).

For L2-L3 larvae (Figure 1B), the nibbling of PE was difficult to observe and LDPE consumption was estimated by weighing the remaining PE (Supporting Information Table 1). The larval weight uptake was followed up to 16 days. The weight of larvae fed with a pollen–beeswax diet increased 10 times, while with a pollen-only diet, it increased 3 times and 1.3 times with a beeswax-only diet. The pollen–beeswax diet was the optimal condition for Gm larval growth. The control larvae, without food, died after 3 days. Larvae fed with only LDPE lost weight (1.3-fold), did not change growth stage, and exhibited 50% mortality at day 3 and 100% mortality at day 6,

https://doi.org/10.1021/acs.est.1c03417
Environ. Sci. Technol. XXXX, XXX, XXX–XXX

probably due to starvation. Larvae fed with both LDPE and pollen did not gain weight compared to larvae fed only with pollen. This indicated that although they consumed LDPE (Figure 1B), it did not provide energy for growth or survival at early development stages (see detailed diet consumption in Supporting Information Table 1).

For L6 larvae, LDPE consumption was observed directly on colored and not-colored commercial LDPE films. Residues of colored PE were found in the excreted feces (Figure 1C). We followed the growth of L6 stage larvae fed with different diets for 7 days (Figure 1D and Supporting Information Table 2). The results demonstrate that—as for the young larvae—the best diet was a combination of beeswax and pollen, since the larvae almost doubled weight in 7 days. Larvae fed with a pollen-only diet, wax-only diet, or LDPE−pollen diet survived but did not gain weight. Larvae fed with LDPE-only diet lost 25% of their weight as did the control larvae (no food), but all survived and were able to complete metamorphosis into a moth, like in all the other conditions. In average, larvae fed with a pollen−PE diet had each consumed 0.48 mg PE/day/larva, and larvae fed with a PE-only diet consumed 0.37 mg PE/day/larva; these rates are comparable to those reported by Lou[18] (0.60 mg PE/day/larva) but inferior to those reported by Bombelli[11] (1.84 mg PE/day/larva).

These experiments show that conventional Gm larvae ingest PE but cannot derive nutritional value from it.

Hyperspectral Infrared Imaging of Larva Cryo-sections. Although the larvae did not gain weight by eating PE in the aforementioned experiment, it does not prove that Gm larvae or their microbiota could not metabolize small quantities of this PE. Therefore, we developed a method based on μFTIR[26,27] hyperspectral imaging for measuring the chemical composition of the Gm larvae tissues. The ultimate goal was to detect the presence of metabolized PE in the tissue following ingestion of deuterated PE.

First, we set up the μFTIR hyperspectral imaging experiment to measure the spectral tissue composition (sugars, proteins, and lipids) and if deuterium can be detected in Gm larvae thin sections in larvae fed with an optimal pollen and wax diet. Hyperspectral infrared images of 10 μm thick cryo-sections of control larvae were recorded (Figure 2A−E). The spectra and peak area used to generate the spectral maps are shown in Figure 2L and Supplementary Figure S1. Representative spectra from different tissues were obtained by classifying all the larval tissue spectra in 4 groups by k-means clustering (Supporting Information Figure S1A). The IR absorption spectra from the larval tissues were typical biological tissue spectra.[28] They were dominated by the absorption bands of the stretching vibration of O−H and N−H bonds present in sugars and proteins at 3400 and 3300 cm^{-1}; C−H peaks from lipids and proteins between 3020 and 2800 cm^{-1}; C═O peaks from esterified lipids at 1740 cm^{-1} and carboxylic acids at 1710 cm^{-1}; CONH peaks from proteins at 1654 and 1545 cm^{-1}; C−H and COOH peaks between 1480 and 1350 cm^{-1}; P═O peaks at 1240 and 1080 cm^{-1}; and C−OH, C−OP, COC, and COH peaks from carbohydrates and lipids at 1160, 1150, 1100, 1035, and 1025 cm^{-1}. While proteins peaks are generally the most intense peaks in the spectra of most animal tissues, peaks from phospholipids and esterified lipids (C−H, C═O, C−OC, and C−OP) strongly dominated the spectra of larva tissues showing their extremely high lipid concentration. The C═C−H olefinic peak from unsaturated lipids at 3008 cm^{-1} was detected in the lipid-rich tissues, evidencing a strong lipid unsaturation level. In Figure 2B,C, we present respectively the protein and lipid distribution from the control larva section shown in Figure 2A. Silk glands and some epithelial regions (evidenced by the amide I band at 1650 cm^{-1}) appeared, like a red hotspot in the protein image, while fatty tissues (evidenced by esterified lipids by the ester C═O peak at 1740 cm^{-1}) appeared red in the lipid image.

No deuterium could be detected in control larvae by looking at the 2000−2200 cm^{-1} range that contains the strongest C−D stretching peaks. Figure 2D,E shows hyperspectral maps of the larva cryo-section at 2197 and 2098 cm^{-1}, respectively, evidencing the absence of detectable C−D peaks in the control larvae. The faint tissue contours observed in Figure 2E arise from baseline drifts caused by IR radiation scattering at the edge of the tissue and not from the C−D peak. The typical C−D peaks are shown in Supporting Information Figure S1B in the spectrum of deuterated PED4 (red) and of deuterated oil (green) dominated by the C−D stretching peak at 2197 and 2098 cm^{-1}, shown along with the spectrum of a normal PE film (blue) dominated by the methylene ($-CH_2-$) peaks at 2914 and 2848 cm^{-1}. This shows that deuterium at natural abundance is not detectable even in the fatty larval tissue since natural concentrations are in the parts per million range,[29] well below the detection limits of μFTIR.

Detection of Deuterium in Cryo-sections of Larva Fed with Deuterated Oil. In order to prove that deuterium could be detected (as C−D bonds) in larvae that had ingested deuterated food, conventional and axenic larvae were fed during 24 and 72 h with $C_{16}D_{34}$ perdeuterated oil. The oil was mixed with pollen to facilitate its ingestion since larvae would not ingest pure oil. On average each larva had ingested 1.4 mg of oil in 24 h and 4.2 mg in 72 h. The larvae were then cryo-sectioned, and the thin sections were investigated by μFTIR (Figure 2F−K). A weak C−D signal could be detected after 24 h, at discrete locations (not shown), but the C−D signal was consistently detected in most tissues after 72 h of feeding (Figure 2I,J). This suggests that the threshold for consistent detection was around 2 to 2.5 mg of ingested deuterated food. The C−D signal was detected at discrete locations throughout the sections and appeared stronger in some lipid rich tissues. The related spectra can be seen in Supporting Information Figure S1C showing the pure $C_{16}D_{34}$ oil spectrum and the spectra from the different larval tissues. We found a moderately positive correlation between the distribution of lipids and deuterated molecules with a correlation coefficient of 0.42 between the C−D and C−H signals. This confirmed that deuterated food assimilation could be detected more sensitively in the fat tissues. Figure 2K shows a zoom on a C−D-rich region, and the spectra are shown in Supporting Information Figure S1D. The C−D signal measured with the μFTIR imaging system was low, with a maximum of 0.025 a.u. at 2197 cm^{-1} in the hot spot shown in Figure 2K. We used a confocal microscope coupled to a synchrotron source to improve measurement sensitivity and accuracy (Figure S1E) and measured a one order of magnitude higher C−D signal (up to 0.20 A.U.) than with the imaging system. The synchrotron data were then used to examine if the oil was changed upon metabolization: the CD_2 peak position (sensitive to the molecule environment) and the CD_2/CD_3 ratio (related to the aliphatic chain length) were determined and compared in the pure oil and in the deuterated fatty tissues. The CD_2/CD_3 ratio measured at 24 different positions in the larval tissue varied between 0.72 and 3.6 (mean 2.16)

https://doi.org/10.1021/acs.est.1c03417
Environ. Sci. Technol. XXXX, XXX, XXX−XXX

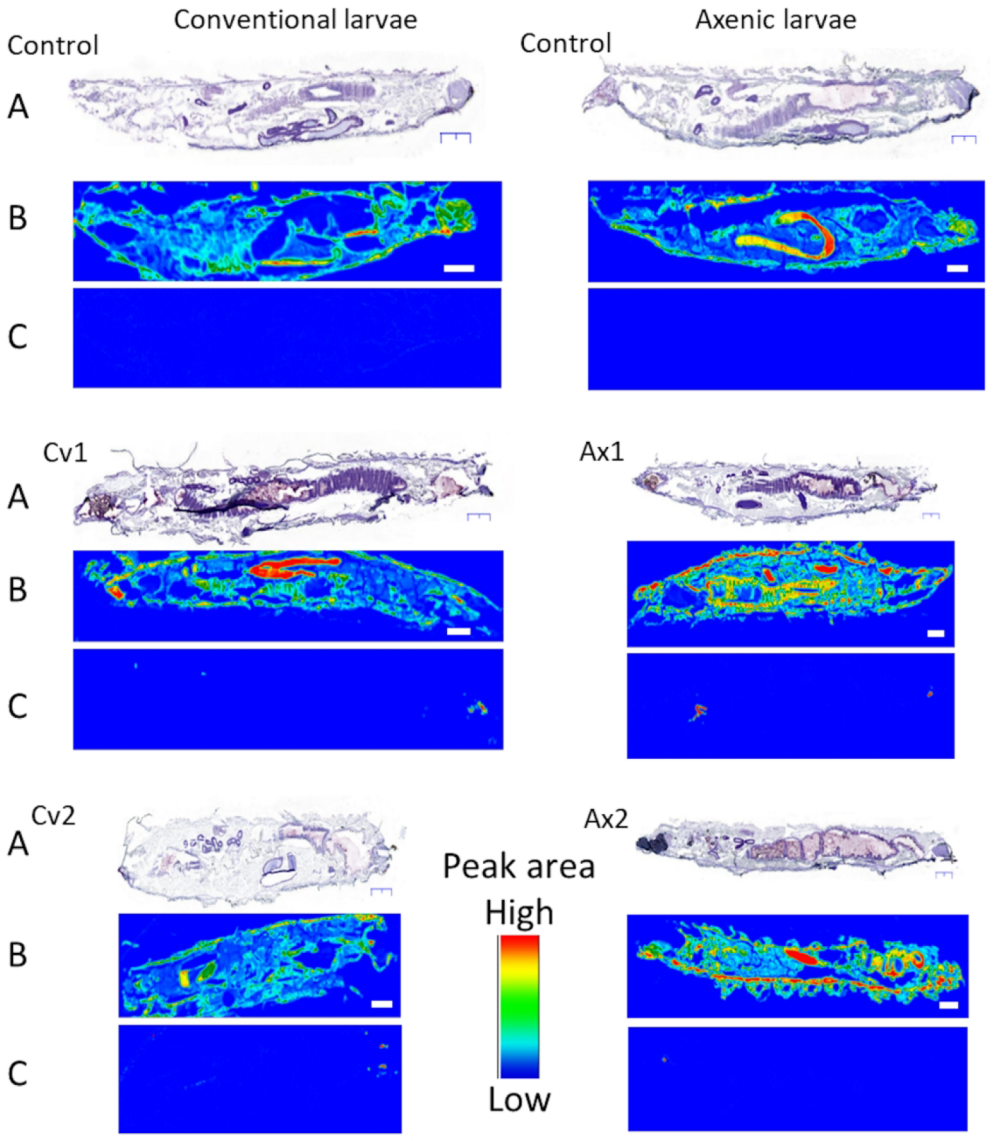

Figure 3. Presence of the C−D signal in Gm larvae fed with PED4. Conventional (Cv) and axenic (Ax) control larvae were fed with nondeuterated PE for 3 days, and test larvae were fed with deuterated PE for 3 days (Cv1 and Ax1). Cv2 and Ax2 larvae were fed with alternating diets (see Materials and Methods) over a period of 19 days. Sections were stained with cresyl violet and observed in bright field microscopy (A) or kept unstained and analyzed by μFTIR (B and C). The IR hyperspectral images show the distribution of (B) proteins (1650 cm^{-1} amide I peak area) and (C) deuterated PE (2197 cm^{-1} C−D peak area). No deuterated molecules were found in the tissue of the conventional and axenic control larvae or in the Cv1, Ax1, Cv2, and Ax2 larvae, but few deuterated PE particles were detected in the mouth, gut, and rectum of both Cv and Ax larvae. Spectra from such particles are shown in Figure S1F. Scale bar: 1 mm and magnification was 4× in both IR and visible micrographs.

and was different from its value in the pure oil (1.92) showing that the oil was fragmented and CD_2 moieties were integrated in shorter and in longer aliphatic chains. This supported the idea of metabolization of the oil in the larva. The CD_2 peak positions in pure oil and in the tissues were not significantly different at 2197.1 ± 1.2 cm^{-1} and 2197.3 ± 0.4 cm^{-1}, respectively (student $p > 0.05$). The positions of the C−D peaks are sensitive to the conformation of lipids to their local environment and to the long-range order such as the organization in amorphous gel or liquid crystal.[30] This showed that the deuterated lipids were in similar environments in the pure oil and in the tissues, probably as small droplets, and that the differences in CD_2/CD_3 ratio were not due to local environment changes.

These results clearly demonstrate that the larvae were able to metabolize and integrate deuterated food into their fatty tissue and that μFTIR hyperspectral imaging is sensitive enough to detect the metabolization of a few milligrams of deuterated food.

Investigations into Cryo-sections of Larva Fed with Deuterated PE. Therefore, we then investigated whether Gm larvae fed with deuterated PE (PED4) were able to assimilate PE by seeking the appearance of C−D peaks in the larval tissues. Similarly, we recorded hyperspectral infrared images from sections from 5 conventional and 5 axenic L6 larvae fed for 3 days with PED4 and 2 conventional and 2 axenic control larvae fed with nondeuterated PE. For each larva, two cryo-sections, one 10 μm thick and one 20 μm thick, were analyzed. Each larva ingested on average 2.1 mg of PED4 (min 1 mg, max 4 mg) or 0.7 mg of PED4/day/larva for L6 larvae. This rate is similar to that of normal LDPE and to those reported in the literature by Lou et al.[18] Three additional L3 larvae were

https://doi.org/10.1021/acs.est.1c03417
Environ. Sci. Technol. XXXX, XXX, XXX−XXX

fed for 19 days with PED4 alternating with a pollen diet to keep them alive and ate 3.6 mg of PED4 on average. This was comparable to the quantities of deuterated oil ingested by the larvae (1.4 mg and 4.2 mg at 24 and 72 h, respectively).

The results are presented in Figure 3, which shows visible and IR hyperspectral images of one representative larval cryosection for each condition. IR hyperspectral images of the protein peak at 1650 cm^{-1} and CD_2 peak at 2197 cm^{-1} are shown. In the control axenic and conventional larvae, no absorption of C−D could be detected in the tissues, as expected. No C−D peak was detected in the tissues of the 5 conventional and 5 axenic larvae fed for 3 days with PED4. To ensure that it was not due to a sensitivity issue, 20 μm thick sections were studied, giving the same results. In order to further boost the sensitivity of the method, another set of conventional and axenic L3 stage larvae were fed during 12 to 19 days with PED4. To make sure that the larvae could survive over 6 days with this low nutritional value diet, the 12- and 19-days periods were fractioned in periods of 3 days alternating between the PED4-only diet and PED4 plus pollen diet. These L3 larvae had consumed 3.6 ± 1.1 mg PED4 per larva at the end of the experiment at rates of 0.19 to 0.28 mg PED4/day/larva (L3 larvae eat less than L6 larvae).

No C−D peak was detected in the tissues of these L3 larvae (Cv2 and Ax2 in Figure 3).

However, particles with a C−D signal were detected in cavities of the digestive tract such as the mouth, the gut, and the rectum in 6 out of 10 of the conventional and axenic larvae fed with PED4. This corresponded to the presence of micrometer sized PED4 particles (25−50 μm) and aggregates (up to 1000 μm). The larger PED4 particles were observed in the oral cavity and rectum. No differences were observed between axenic and conventional larvae. The particles appeared more numerous in the mouth and rectum, and fewer particles were found in the gut. Since no embedding was used, it is possible that some of the gut particles were lost during sectioning. While the largest particles could be detected by microscopic observation, the C−D IR signature allowed detecting smaller particles. The spectral signature also allowed confirming the chemical nature of the particles. To investigate whether smaller particles present in the gut could escape detection with hyperspectral imaging, we also recorded SR-μFTIR maps and were able to detect micrometer-sized PE particles in the gut of the larvae (Figure S1F). We also tried to evaluate whether the PED4 found in the digestive tract was oxidized by analyzing the CD_2/CD_3 ratio of the gut particles using the SR-μFTIR data. However, most particles were either too thick or too scattered to yield good quality spectra that could be used for such analysis.

Biodegradation of PE by Gm Larvae. The absence of PE bioassimilation could be due to an inability of our Gm larva population to biodegrade PE. We investigated this ability by using two methods: detection of PE oxidation by μFTIR imaging of HDPE films in contact with the dissected guts of Gm larvae and analysis of the CD_2/CD_3 ratio of PED4 particles in the Gm larval frass by ATR-FTIR. The results are detailed in the Supporting Information.

Weak PE oxidation was detected in the PE films in contact with the guts of conventional Gm larvae (Figure S2) by μFTIR imaging but not with guts from the axenic larvae. Meanwhile the results did not allow us to make a conclusion on the implication of the Gm microbiota since variations were found among the replicates of axenic larvae.

The CD_2/CD_3 ratio of PED4 particles in the gut of the larvae was measured by ATR-FTIR in the excreted larval frass (Supporting Information). It was found to be 15% lower for the PED4 particles in the frass (2.91 ± 0.32) than for the pristine PED4 films (3.42 ± 0.40), suggesting shorter aliphatic chains in the digested PED4, thus indicating some chemical modification and biodegradation of PED4 (Figure S3) in the gut.

DISCUSSION

The capability of Gm larvae to digest and bioassimilate PE is controversial[11,12,14,16,19,31] and necessitates further investigation. The role of the Gm microbiota is also disputed.[12,14,18] We therefore examined whether the Gm larvae with and without microbiota were only chewing PE or were truly able to digest and metabolize it.

Feeding experiments showed that pollen+beeswax was the optimal diet, in agreement with literature.[14,17] Early larval stages L2-L3 fed with PE lost weight and died in 3 days (50%) to 10 days (100%). This trend is similar to results from Lou et al. (50% death at 15 days).[18] Kong et al. reported 100% survival but 20−30% weight loss in PE-fed Gm larvae in 14 days.[14] Billen et al. reported that an LDPE diet was not sufficient for sustaining Gm larva growth.[31] Lemoine et al. reported a 50% weight loss on a PE diet.[32] Our results suggested that a pollen-only diet is sufficient for the survival of the larvae and that an additional source of carbon such as beeswax allows larvae to gain weight, in agreement with the literature.[17,14] L2-L3 larvae fed with pollen and PE survived 16 days and gained some weight but far less than the larvae fed with the optimal diet.

This trend was confirmed with the last stage (L6) larvae fed only with PE as they lost weight compared to larvae fed with pollen or beeswax and consumed 80 times less food than larvae fed with beeswax. We did not observe significant differences in feeding behavior or weight gain between conventional and axenic larvae, suggesting that the microbiota may not be important for their development and life cycle under our conditions and those reported by Kong.[14] For L6 larvae, the final life cycle was similar for Gm larvae fed with PE or beeswax: after 8 days the larvae pupated, the adult moths appeared 1 week later, and egg production was similar. These experiments showed that PE does not have nutritional value for the Gm larvae. Larvae at the early L6 stage have accumulated enough reserves to continue their life cycle even if their diet is changed to PE alone, whereas larvae at an early stage cannot survive with PE alone.

We then evaluated whether PE could be bioassimilated by Gm larva. We developed a new approach based on the μFTIR hyperspectral imaging of carbon−deuterium bonds in cryosections of larvae fed with deuterated PE. This method could, potentially, not only allow showing the metabolization of PE but also help find in which tissues PE metabolites accumulate and what kind of biomolecules might be synthesized using PE. We first established that it was possible to detect the metabolization of deuterated food in the tissues of larvae fed with perdeuterated oil mixed with pollen: the C−D signal was indeed detected in most tissues and predominantly in fatty tissues (adipocytes) after a 3 day diet in both axenic and conventional larvae. The CD_2/CD_3 peak area ratio was modified compared to the original oil signal showing that the oil was integrated in shorter and in longer aliphatic chains. This demonstrated that μFTIR could detect the C−D signal in

https://doi.org/10.1021/acs.est.1c03417
Environ. Sci. Technol. XXXX, XXX, XXX−XXX

tissue sections from larvae that had ingested and metabolized 1 to 4 mg of deuterated food.

On the contrary, we could not detect any C−D signal in L6 larvae fed with PED4 during 3 days or during 19 days. The absence of the C−D signal indicated that the PE was not metabolized and integrated in the larvae body in substantial quantities. This should not be due to a lack of sensitivity of the spectroscopic method since the larvae had ingested 2.1 mg of PED4 per larva after 3 days and 3.6 mg of PED4 per larva after 19 days (up to 5 mg), while as discussed above a C−D signal was consistently detected in most tissues when larvae ingested 4.2 mg of deuterated oil. We estimate that the method will allow detecting reliably the assimilation of around 2 mg of deuterated food and even lower quantities with the help of a synchrotron source. Meanwhile, PED4 microparticles were detected in the mouth, gut, and rectum of the larvae, confirming that Gm larvae were able to break and masticate the PE films in smaller, micrometer-sized particles. Instead of metabolizing the plastic, the larvae generated micrometer-sized particles which could be worse for the environment and more difficult to collect than larger pieces of plastic.[31]

Polymer characteristics such as molecular weight, crystallinity, surface hydrophobicity, glass transition temperature, etc. may hamper enzymatic biodegradation. The PED4 used here had a higher average molecular weight (MW) of 821 kDa than the HDPE and LDPE from commercial bags (641 kDa and 249 kDa, respectively). However, all 3 samples presented broad MW distributions ranging from hundreds to millions of Da (Supporting Information Figure S5). HDPE presented a light chain fraction at 150 kDa and a heavy chain fraction at 300 kDa, and the PED4 had a MW distribution similar to this heavier chain fraction and also centered at 300 kDa. PED4 crystallinity (0.9) also fell in the range of commercially available HDPE (0.6−0.9). Thus, the PED4 used in this study can be considered representative of the heavy fraction of commercially available HDPE bags. Since plastic digestibility may strongly depend on PE density, the next steps could be to investigate the bioassimilation of deuterated LDPE with lighter molecular weights, which could theoretically show better bioassimilation.

Yang et al.[33] observed negligible integration of ^{13}C in the body of the beetle larvae of *Tenebrio molitor* Linnaeus fed with ^{13}C polystyrene (PS) and found that a large fraction of the ^{13}C was integrated in the CO_2 produced by the gut bacteria. Recently, independent results of Cassone et al.[16] and Ren et al.[12] reported that bacteria isolated from the Gm larva gut were able to grow on and degrade PE into smaller compounds, implicating a role of the gut microbiota. Our results showed no PE bioassimilation in either axenic or conventional larvae. Since our Gm population was able to survive on beeswax, develop on beeswax−pollen, and assimilate perdeuterated oil, it does possess the required enzymes to efficiently metabolize long- and short-length hydrocarbons. The absence of bioassimilation even in conventional larvae with an intact microbiota might indicate that our Gm population lacked some of the bacterial species/strains capable of degrading PE in smaller hydrocarbons that were present in other Gm populations described in the literature. However, we found weak oxidation in PE films in contact for 24 h with the dissected gut of conventional larvae and a shortening of aliphatic chains in PED4 particles excreted in the larval frass, indicating that a PE oxidation capability exists in our Gm. The oxidation of PE in the larval gut could favor its biodegradation even in the absence of bioassimilation since oxidation is the first step of environmental biodegradation. Several groups reported isolating bacterial and fungal strains capable of digesting PE from different Gm populations: Cassone reported isolating an *Acinetobacter* sp. from Gm,[16] while Ren reported isolating an *Enterobacter* sp,[12] and Zhang reported isolating an *Aspergillus flavus* strain.[34] Yang isolated strains of *Bacillus* sp. and *Enterobacter* sp. able to digest PE from the Gm related *P. interpunctella* larvae.[35] The microbiota of our Gm population was analyzed by 16S rRNA gene sequencing and was shown to be composed of mainly Firmicutes (*Enterococcus*) and a lower amount of Cyanobacteria and Proteobacteria, (Supporting Information Figure S4). The Proteobacteria were mostly *Enterobacteriaceae*, although *Acinetobacter* sp. was absent, and the amount of proteobacteria was low. The *Enterococcus* species in our Gm population suggested that its microbiota was not fundamentally different from those reported by other groups.[18] In microbial biodegradation studies, most of the identified bacteria belong to the Proteobacteria (48%) and Firmicutes (37.4%),[36] which are also present in our Gm microbiota. We will investigate the PE-degrading capacity of the Gm microbiota. FTIR microspectroscopy could be used to measure the integration of C−D in microcolonies of bacteria grown on PED4 films and will be tested in our follow-up work.

■ ASSOCIATED CONTENT

Supporting Information

The Supporting Information is available free of charge at https://pubs.acs.org/doi/10.1021/acs.est.1c03417.

Average food consumptions by L3 stage larvae (average consumed weight per individual larva for 16 days); average food consumptions by L6 stage larvae (average consumed weight per individual larva for 7 days); infrared spectra of the larval tissues, of normal polyethylene and deuterated polyethylene, as film or as particles found in the gut of larvae, and of the deuterated oil used in this study in pure form and as found in the larval tissues; results of the biodegradation of HDPE films by the dissected gut of Gm larvae; evaluation of PE oxidation after contact for 24 h with the guts of Gm larvae; alteration of PED4 in the gut of the Gm larvae evaluated by a change in the CD2/CD3 ratio directly in the spectra of Gm larvae feces; analysis of Gm larva microbiota by 16S rRNA sequencing; evaluation of the crystallinity index of the various PE used in this study by IR spectroscopy; and molecular weight distributions of the PE used in this study (PDF)

■ AUTHOR INFORMATION

Corresponding Authors

Agnès Réjasse − *Université Paris-Saclay, INRAE, AgroParisTech, Micalis Institute, 78350 Jouy-en-Josas, France*; Email: agnes.rejasse@inrae.fr

Christophe Sandt − *SMIS beamline, Synchrotron Soleil, L'Orme des Merisiers, 91192 Cedex Gif-sur-Yvette, France*; orcid.org/0000-0002-6432-2004; Email: sandt@synchrotron-soleil.fr

Authors

Jehan Waeytens − *Structure et Fonction des Membranes Biologiques, Université libre de Bruxelles, B-1050 Bruxelles,*

https://doi.org/10.1021/acs.est.1c03417
Environ. Sci. Technol. XXXX, XXX, XXX−XXX

Belgique; Université Paris-Saclay, CNRS, Institut de Chimie Physique, UMR 8000, 91405 Orsay, France

Ariane Deniset-Besseau − *Université Paris-Saclay, CNRS, Institut de Chimie Physique, UMR 8000, 91405 Orsay, France*

Nicolas Crapart − *UMR 1313 GABI, Abridge, INRAE, Université Paris-Saclay, 78350 Jouy en Josas, France; Exilone, 78990 Elancourt, France*

Christina Nielsen-Leroux − *Université Paris-Saclay, INRAE, AgroParisTech, Micalis Institute, 78350 Jouy-en-Josas, France*

Complete contact information is available at: https://pubs.acs.org/10.1021/acs.est.1c03417

Author Contributions

A.R. initiated the study, designed the research, reared the insects, performed insect feeding experiments, and participated in the writing of the manuscript. J.W. performed infrared microspectroscopy measurements, prepared figures, and participated in the writing of the manuscript. A.D.-B. participated in the study design and corrected the manuscript. N.C. performed insect cryo-section and tissue coloration. C.N.-L. participated in the study design and corrected the manuscript. C.S. designed the infrared microspectroscopy study, performed the infrared microspectroscopy measurements, prepared figures, and wrote the manuscript.

Notes

The authors declare no competing financial interest.

■ ACKNOWLEDGMENTS

The authors acknowledge the Synchrotron SOLEIL for provision of synchrotron radiation facilities and FTIR microspectroscopy equipment. The authors also acknowledge the INRAE-Jouy-en-Josas histology platform (Abridge) for the cryo-sectioning and microscopy facilities and the INRAE-MICA department for the general support to C.N.-L. and A.R. The authors acknowledge Stéphane Chaillou from INRAE-MICALIS team FME for deciphering the Gm microbiota using 16SRNA gene sequencing and for useful discussion. The authors wish to acknowledge DIM-ACAV from Région Ile de France for financial support.

■ ABBREVIATIONS

Gm, *Galleria mellonella*; PE, polyethylene; LDPE, low density PE; PED4, perdeuterated polyethylene; IR, infrared; FTIR, Fourier transform infrared; μFTIR, FTIR microspectroscopy

■ REFERENCES

(1) Geyer, R.; Jambeck, J. R.; Law, K. L. Production, Use, and Fate of All Plastics Ever Made. *Sci. Adv.* **2017**, *3* (7), e1700782 DOI: 10.1126/sciadv.1700782.

(2) Tokiwa, Y.; Calabia, B.; Ugwu, C.; Aiba, S. Biodegradability of Plastics. *Int. J. Mol. Sci.* **2009**, *10* (9), 3722−3742.

(3) Yamada-Onodera, K.; Mukumoto, H.; Katsuyaya, Y.; Saiganji, A.; Tani, Y. Degradation of Polyethylene by a Fungus, Penicillium Simplicissimum YK. *Polym. Degrad. Stab.* **2001**, *72* (2), 323−327.

(4) Bonhomme, S.; Cuer, A.; Delort, A. M.; Lemaire, J.; Sancelme, M.; Scott, G. Environmental Biodegradation of Polyethylene. *Polym. Degrad. Stab.* **2003**, *81* (3), 441−452.

(5) Yoshida, S.; Hiraga, K.; Takehana, T.; Taniguchi, I.; Yamaji, H.; Maeda, Y.; Toyohara, K.; Miyamoto, K.; Kimura, Y.; Oda, K. A Bacterium That Degrades and Assimilates Poly(Ethylene Terephthalate). *Science (Washington, DC, U. S.)* **2016**, *351* (6278), 1196−1199.

(6) Restrepo-Flórez, J. M.; Bassi, A.; Thompson, M. R. Microbial Degradation and Deterioration of Polyethylene - A Review. *Int. Biodeterior. Biodegrad.* **2014**, *88* (March), 83−90.

(7) Yang, Y.; Yang, J.; Wu, W. M.; Zhao, J.; Song, Y.; Gao, L.; Yang, R.; Jiang, L. Biodegradation and Mineralization of Polystyrene by Plastic-Eating Mealworms: Part 2. Role of Gut Microorganisms. *Environ. Sci. Technol.* **2015**, *49* (20), 12087−12093.

(8) Yang, Y.; Wang, J.; Xia, M. Biodegradation and Mineralization of Polystyrene by Plastic-Eating Superworms Zophobas Atratus. *Sci. Total Environ.* **2020**, *708*, 135233.

(9) Yang, S. S.; Wu, W. M.; Brandon, A. M.; Fan, H. Q.; Receveur, J. P.; Li, Y.; Wang, Z. Y.; Fan, R.; McClellan, R. L.; Gao, S. H.; Ning, D.; Phillips, D. H.; Peng, B. Y.; Wang, H.; Cai, S. Y.; Li, P.; Cai, W. W.; Ding, L. Y.; Yang, J.; Zheng, M.; Ren, J.; Zhang, Y. L.; Gao, J.; Xing, D.; Ren, N. Q.; Waymouth, R. M.; Zhou, J.; Tao, H. C.; Picard, C. J.; Benbow, M. E.; Criddle, C. S. Ubiquity of Polystyrene Digestion and Biodegradation within Yellow Mealworms, Larvae of Tenebrio Molitor Linnaeus (Coleoptera: Tenebrionidae). *Chemosphere* **2018**, *212*, 262−271.

(10) Peng, B. Y.; Su, Y.; Chen, Z.; Chen, J.; Zhou, X.; Benbow, M. E.; Criddle, C. S.; Wu, W. M.; Zhang, Y. Biodegradation of Polystyrene by Dark (Tenebrio Obscurus) and Yellow (Tenebrio Molitor) Mealworms (Coleoptera: Tenebrionidae). *Environ. Sci. Technol.* **2019**, *53* (9), 5256−5265.

(11) Bombelli, P.; Howe, C. J.; Bertocchini, F. Polyethylene Bio-Degradation by Caterpillars of the Wax Moth Galleria Mellonella. *Curr. Biol.* **2017**, *27* (8), R292−R293.

(12) Ren, L.; Men, L.; Zhang, Z.; Guan, F.; Tian, J.; Wang, B.; Wang, J.; Zhang, Y.; Zhang, W. Biodegradation of Polyethylene by Enterobacter Sp. D1 from the Guts of Wax Moth Galleria Mellonella. *Int. J. Environ. Res. Public Health* **2019**, *16* (11), 1941.

(13) Kundungal, H.; Gangarapu, M.; Sarangapani, S.; Patchaiyappan, A.; Devipriya, S. P. Efficient Biodegradation of Polyethylene (HDPE) Waste by the Plastic-Eating Lesser Waxworm (Achroia Grisella). *Environ. Sci. Pollut. Res.* **2019**, *26* (18), 18509−18519.

(14) Kong, H. G.; Kim, H. H.; Chung, J.; Jun, J. H.; Lee, S.; Kim, H. M.; Jeon, S.; Park, S. G.; Bhak, J.; Ryu, C. M. The Galleria Mellonella Hologenome Supports Microbiota-Independent Metabolism of Long-Chain Hydrocarbon Beeswax. *Cell Rep.* **2019**, *26* (9), 2451−2464.e5.

(15) Kundungal, H.; Gangarapu, M.; Sarangapani, S.; Patchaiyappan, A.; Devipriya, S. P. Role of Pretreatment and Evidence for the Enhanced Biodegradation and Mineralization of Low-Density Polyethylene Films by Greater Waxworm. *Environ. Technol.* **2021**, *42*, 717.

(16) Cassone, B. J.; Grove, H. C.; Elebute, O.; Villanueva, S. M. P.; LeMoine, C. M. R. Role of the Intestinal Microbiome in Low-Density Polyethylene Degradation by Caterpillar Larvae of the Greater Wax Moth. *Proc. R. Soc. London, Ser. B* **2020**, *287* (1922), 20200112.

(17) Roy, D. N. On the Nutrition of Larvae of Bee-Wax Moth, Galleria Mellonella. *J. Comp. Physiol., A* **1937**, *24* (5), 638−643.

(18) Lou, Y.; Ekaterina, P.; Yang, S. S.; Lu, B.; Liu, B.; Ren, N.; Corvini, P. F. X.; Xing, D. Biodegradation of Polyethylene and Polystyrene by Greater Wax Moth Larvae (Galleria Mellonella L.) and the Effect of Co-Diet Supplementation on the Core Gut Microbiome. *Environ. Sci. Technol.* **2020**, *54* (5), 2821−2831.

(19) Weber, C.; Pusch, S.; Opatz, T. Polyethylene Bio-Degradation by Caterpillars? *Curr. Biol.* **2017**, *27*, R744−R745.

(20) Sandt, C.; Waeytens, J.; Deniset-Besseau, A.; Nielsen-Leroux, C.; Réjasse, A. Use and Misuse of FTIR Spectroscopy for Studying the Bio-Oxidation of Plastics. *Spectrochim. Acta, Part A* **2021**, *258*, 119841.

(21) Hagemann, H.; Snyder, R. G.; Peacock, A. J.; Mandelkern, L. Quantitative Infrared Methods for the Measurement of Crystallinity and Its Temperature Dependence: Polyethylene. *Macromolecules* **1989**, *22* (9), 3600−3606.

(22) Poirier, S.; Rué, O.; Peguilhan, R.; Coeuret, G.; Zagorec, M.; Champomier-Vergès, M. C.; Loux, V.; Chaillou, S. Deciphering Intra-Species Bacterial Diversity of Meat and Seafood Spoilage Microbiota Using GyrB Amplicon Sequencing: A Comparative Analysis with 16S

RDNA V3-V4 Amplicon Sequencing. *PLoS One* **2018**, *13* (9), e0204629.
(23) Dumas, P.; Polack, F.; Lagarde, B.; Chubar, O.; Giorgetta, J. L.; Lefrançois, S. Synchrotron Infrared Microscopy at the French Synchrotron Facility SOLEIL. *Infrared Phys. Technol.* **2006**, *49* (1−2), 152−160.
(24) Demšar, J.; Curk, T.; Erjavec, A.; Hočevar, T.; Milutinovič, M.; Možina, M.; Polajnar, M.; Toplak, M.; Starič, A.; Stajdohar, M.; Umek, L.; Zagar, L.; Zbontar, J.; Zitnik, M.; Zupan, B. Orange: Data Mining Toolbox in Python. *J. Mach. Learn. Res.* **2013**, *14*, 2349−2353.
(25) Toplak, M.; Birarda, G.; Read, S.; Sandt, C.; Rosendahl, S. M.; Vaccari, L.; Demšar, J.; Borondics, F. Infrared Orange: Connecting Hyperspectral Data with Machine Learning. *Synchrotron Radiat. News* **2017**, *30* (4), 40−45.
(26) Miller, L. M.; Dumas, P. From Structure to Cellular Mechanism with Infrared Microspectroscopy. *Curr. Opin. Struct. Biol.* **2010**, *20* (5), 649−656.
(27) Sandt, C.; Dionnet, Z.; Toplak, M.; Fernandez, E.; Brunetto, R.; Borondics, F. Performance Comparison of Aperture-Less and Confocal Infrared Microscopes. *J. Spectr. Imaging* **2019**, *8*, a8.
(28) Peng, C.; Kaščáková, S.; Chiappini, F.; Olaya, N.; Sandt, C.; Yousef, I.; Samuel, D.; Dumas, P.; Guettier, C.; Le Naour, F. Discrimination of Cirrhotic Nodules, Dysplastic Lesions and Hepatocellular Carcinoma by Their Vibrational Signature. *J. Transl. Med.* **2016**, *14* (1), 9.
(29) Kselíková, V.; Vítová, M.; Bišová, K. Deuterium and Its Impact on Living Organisms. *Folia Microbiol. (Dordrecht, Neth.)* **2019**, *64*, 673.
(30) Marshall, C.; Javaux, E.; Knoll, a; Walter, M. Combined Micro-Fourier Transform Infrared (FTIR) Spectroscopy and Micro-Raman Spectroscopy of Proterozoic Acritarchs: A New Approach to Palaeobiology. *Precambrian Res.* **2005**, *138* (3−4), 208−224.
(31) Billen, P.; Khalifa, L.; Van Gerven, F.; Tavernier, S.; Spatari, S. Technological Application Potential of Polyethylene and Polystyrene Biodegradation by Macro-Organisms Such as Mealworms and Wax Moth Larvae. *Sci. Total Environ.* **2020**, *735*, 139521.
(32) Lemoine, C. M. R.; Grove, H. C.; Smith, C. M.; Cassone, B. J. A Very Hungry Caterpillar: Polyethylene Metabolism and Lipid Homeostasis in Larvae of the Greater Wax Moth (Galleria Mellonella). *Environ. Sci. Technol.* **2020**, *54* (22), 14706−14715.
(33) Yang, Y.; Yang, J.; Wu, W. M.; Zhao, J.; Song, Y.; Gao, L.; Yang, R.; Jiang, L. Biodegradation and Mineralization of Polystyrene by Plastic-Eating Mealworms: Part 1. Chemical and Physical Characterization and Isotopic Tests. *Environ. Sci. Technol.* **2015**, *49* (20), 12080−12086.
(34) Zhang, J.; Gao, D.; Li, Q.; Zhao, Y.; Li, L.; Lin, H.; Bi, Q.; Zhao, Y. Biodegradation of Polyethylene Microplastic Particles by the Fungus Aspergillus Flavus from the Guts of Wax Moth Galleria Mellonella. *Sci. Total Environ.* **2020**, *704*, 135931.
(35) Yang, J.; Yang, Y.; Wu, W. M.; Zhao, J.; Jiang, L. Evidence of Polyethylene Biodegradation by Bacterial Strains from the Guts of Plastic-Eating Waxworms. *Environ. Sci. Technol.* **2014**, *48* (23), 13776−13784.
(36) Matjašič, T.; Simčič, T.; Medvešček, N.; Bajt, O.; Dreo, T.; Mori, N. Critical Evaluation of Biodegradation Studies on Synthetic Plastics through a Systematic Literature Review. *Sci. Total Environ.* **2021**, *752*, 141959.

https://doi.org/10.1021/acs.est.1c03417
Environ. Sci. Technol. XXXX, XXX, XXX−XXX